Supplementary Information

Nickel-doped ZnO Porous Sea Urchin Nanostructures with Various Amounts of Oxygen Defects for Volatile Organic Compound Detection

Haibo Ren [1, *], Huaipeng Weng [1], Xumeng Dong [1], Dandan Liang [1], Jiarui Huang [2, *] and Sang Woo Joo [3, *]

[1] School of Materials Science and Engineering, Anhui Polytechnic University, Wuhu, Anhui 241000, China

[2] Key Laboratory of Functional Molecular Solids of the Ministry of Education, Anhui Laboratory of Molecule-Based Materials, College of Chemistry and Materials Science, Anhui Normal University, Wuhu, Anhui 241002, China

[3] School of Mechanical Engineering, Yeungnam University, Gyeongsan, Gyeoungbuk, 712749, Republic of Korea

Corresponding authors. Email addresses: renhaibo@ahpu.edu.cn (H.R.);

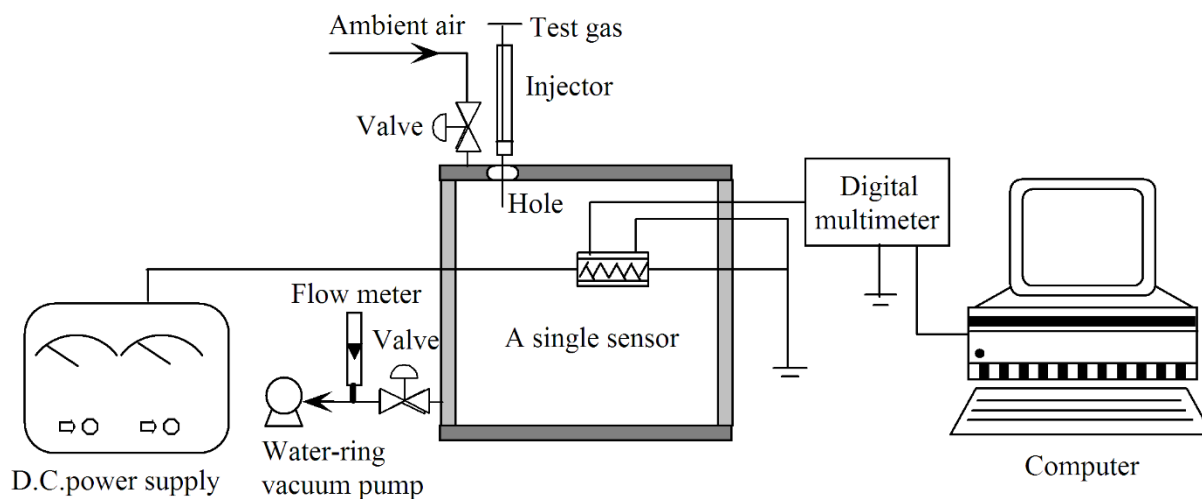jrhuang@mail.ahnu.edu.cn (J.H.); swjoo@yu.ac.kr (S.J.)
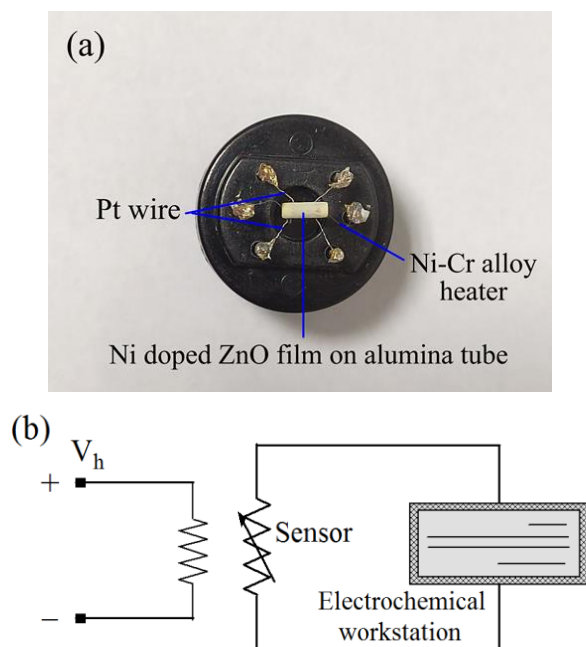
Figure S1. Experimental setup.

Figure S2. (a) Photograph of the sensor and (b) diagram of the testing principle of the gas-sensing measurement system (V_h: heating voltage).
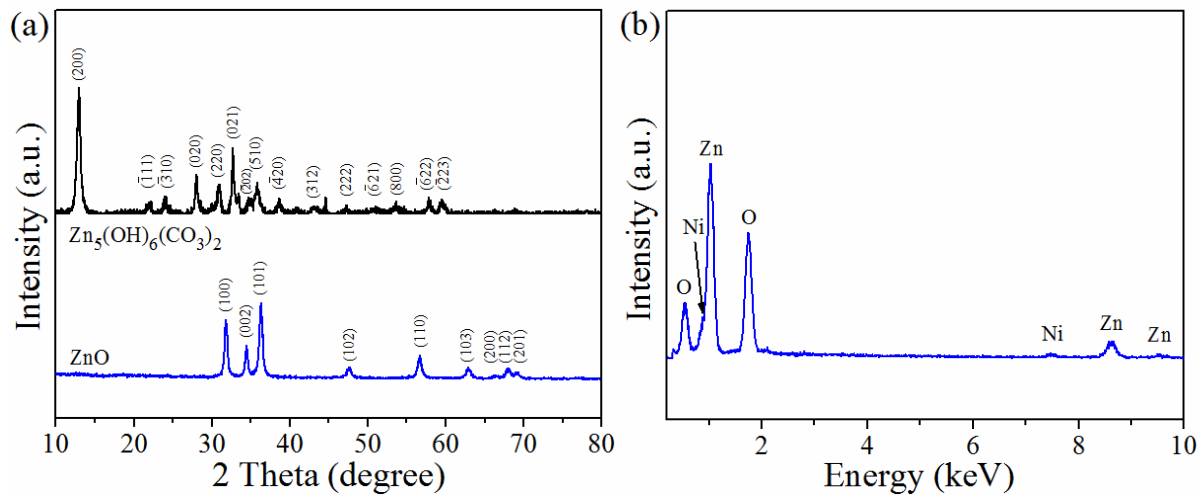
Figure S3. XRD patterns of (a) $Zn_5(CO_3)_2(OH)_6$ precursor and calcined ZnO product, and (b) EDS analysis of 10% Ni-ZnO product.

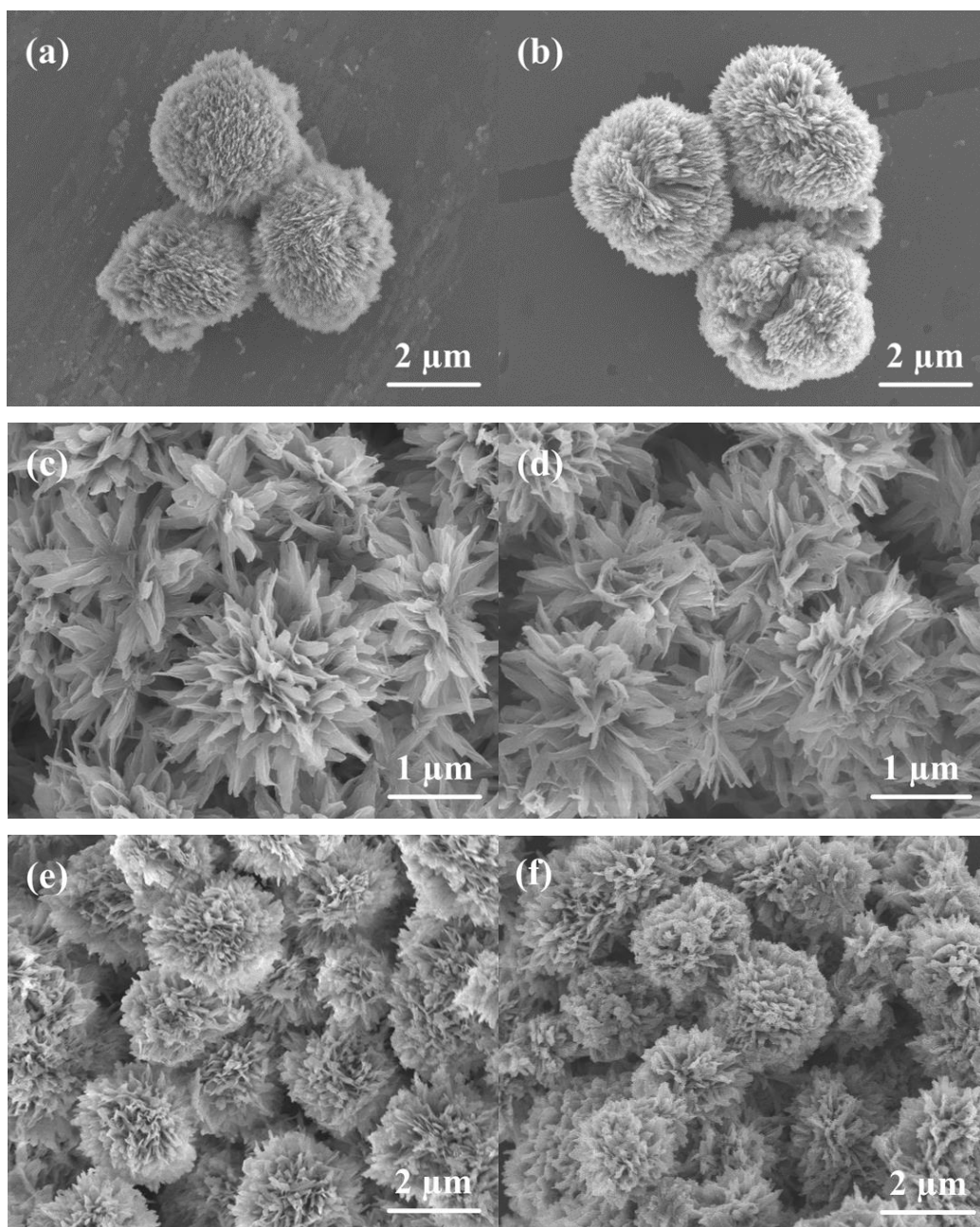**Figure S4.** SEM images of (a) 5% Ni-$Zn_5(CO_3)_2(OH)_6$ precursor and (b) calcined 5% Ni-ZnO product. SEM images of (c) 15% Ni-$Zn_5(CO_3)_2(OH)_6$ precursor and (d) calcined 15% Ni-ZnO product. SEM images of (e) 20% Ni-$Zn_5(CO_3)_2(OH)_6$ precursor and (f) calcined 20% Ni-ZnO product.
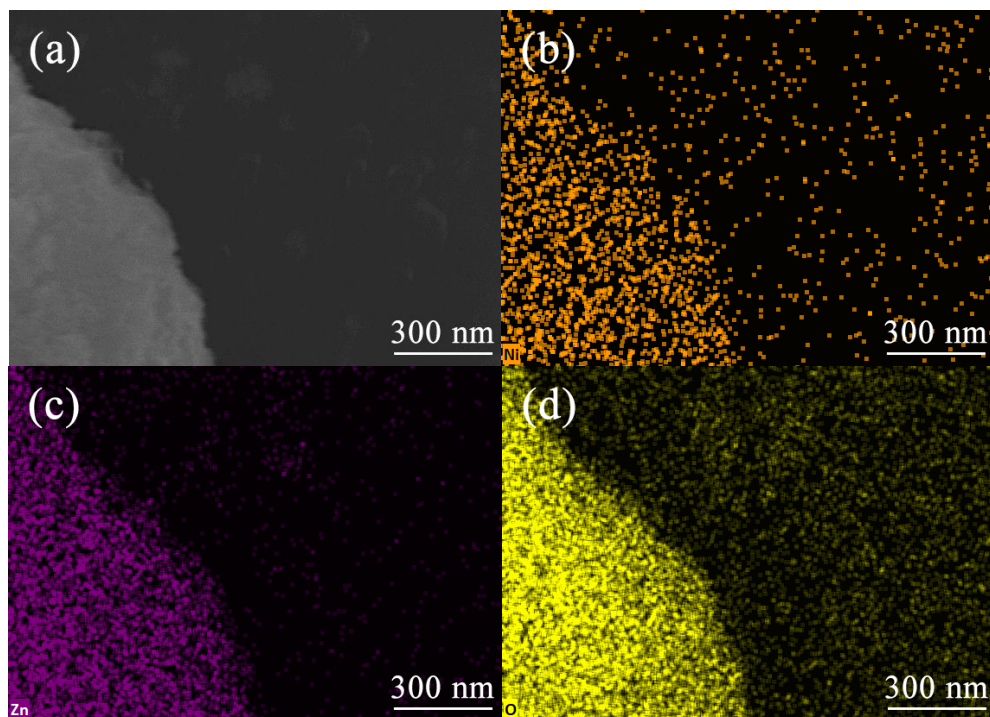
Figure S5. (a) SEM image and corresponding EDS mapping images of the sea urchin-like 10% Ni-ZnO product: (b) Ni, (c) Zn, and (d) O.
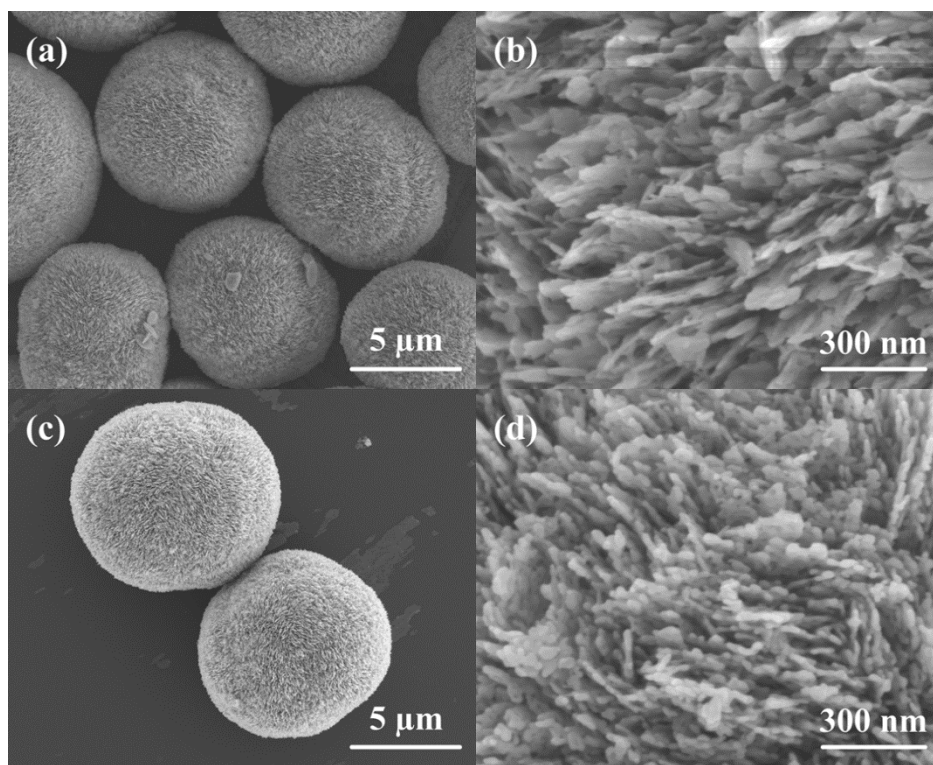

Figure S6. SEM images of (a,b) the $Zn_5(CO_3)_2(OH)_6$ precursor and (c,d) the calcined ZnO product.

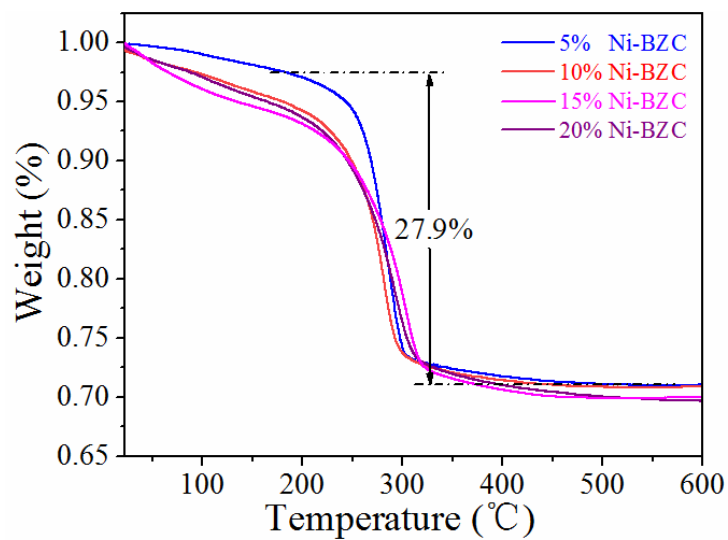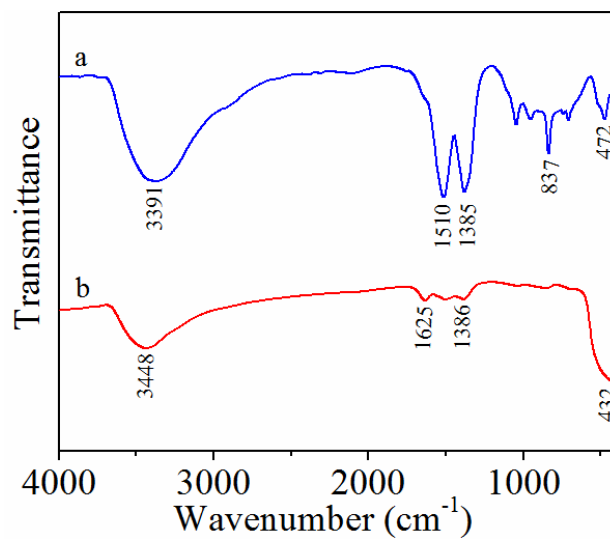**Figure S7.** TGA curves of the sea urchin-like Ni-doped $Zn_5(CO_3)_2(OH)_6$ precursor.

Figure S8. FTIR spectra of (a) the sea urchin-like 10% Ni-$Zn_5(CO_3)_2(OH)_6$ precursor and (b) sea urchin-like 10% Ni-ZnO.
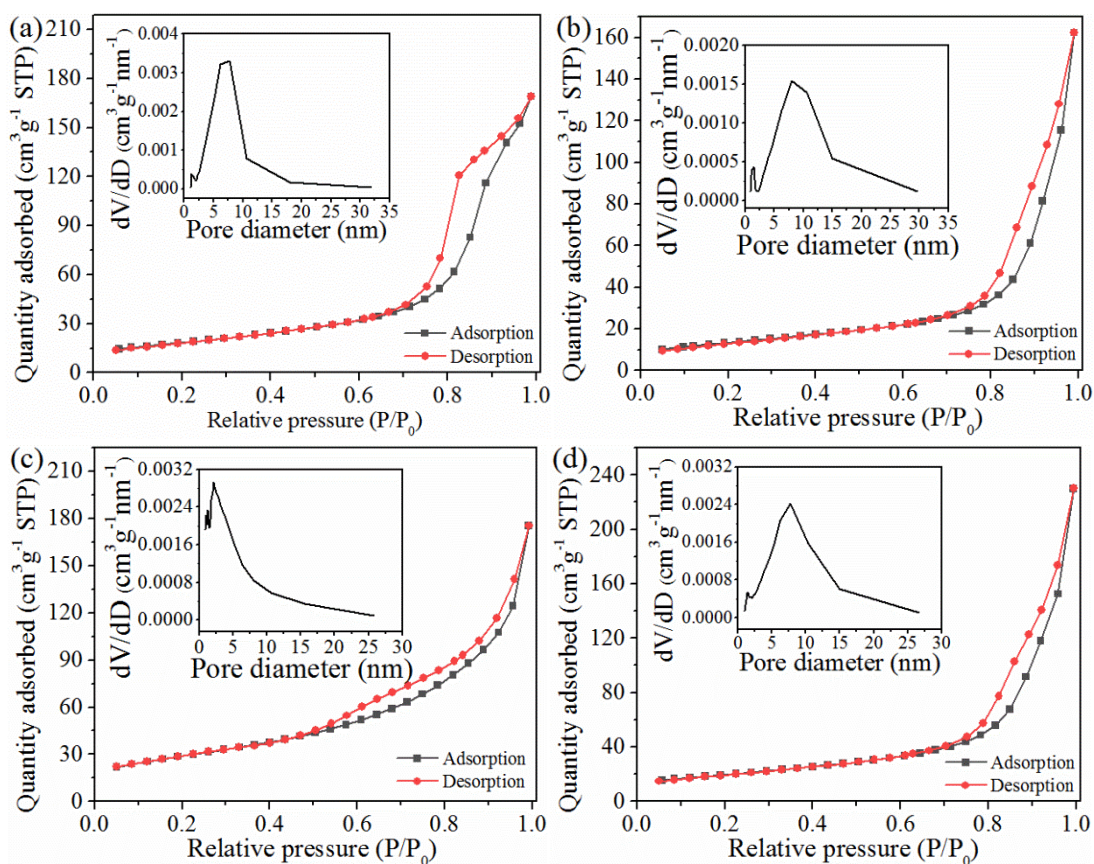
Figure S9. Nitrogen adsorption and desorption isotherms of (a) 5% Ni-ZnO, (b) 10% Ni-ZnO, (c) 15% Ni-ZnO, and (d) 20% Ni-ZnO sea urchins. The insets show the corresponding pore size distributions.

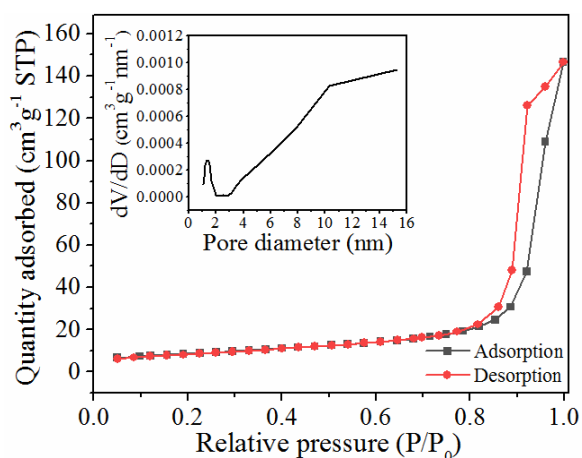**Figure S10.** Nitrogen adsorption–desorption isotherms of pure urchin-like ZnO. The inset is the corresponding pore size distribution.
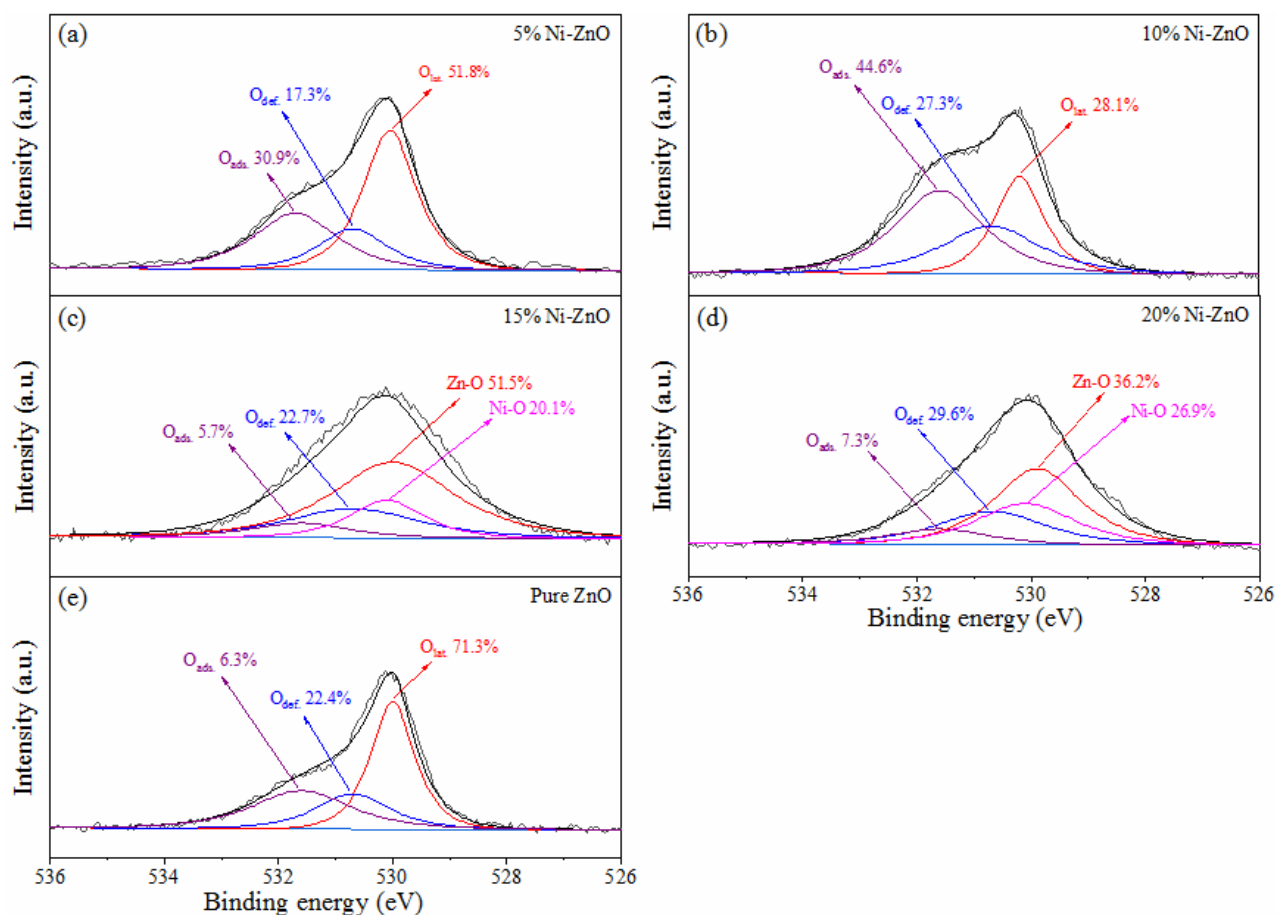
Figure S11. O 1s high-resolution XPS spectrum of (a) 5%, (b) 10%, (c) 15%, and (d) 20% Ni-ZnO sea urchins, and (e) pure ZnO sea urchins.
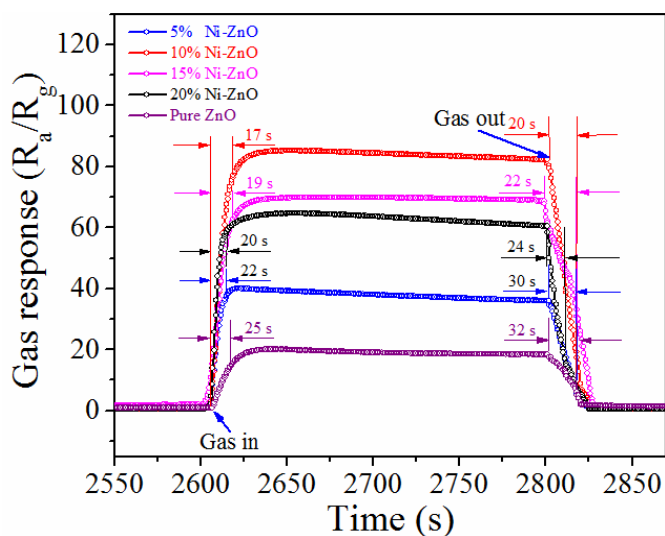

Figure S12. Dynamic response-recovery curves of porous urchin-like Ni-ZnO sensors and the porous urchin-like ZnO sensor towards 100 ppm formaldehyde.

Table S1. Structural parameters of Ni-doped ZnO sea urchins according to the Joint Committee on Powder Diffraction Standards (JCPDS no. 36-1451 (a = 3.250 Å and c = 5.207 Å)).

Samples	Lattice Constants (Å)		Cell volume
	a	c	$V\ (\text{Å}^3)$
0% Ni-ZnO	3.25144	5.20948	47.70
5% Ni-ZnO	3.24733	5.20198	47.51
10% Ni-ZnO	3.24313	5.19258	47.32
15% Ni-ZnO	3.24809	5.21814	47.68
20% Ni-ZnO	3.24740	5.20840	47.57

Table S2. Fitting results of the O 1s XPS spectra of Ni-ZnO and pure ZnO sea urchins.

Sample	Oxygen species	Binding energy (eV)	Relative percentage (%)	$O_{def.}/O_{lat.}$ value
5% Ni-ZnO	$O_{lat.}$	529.9	51.8	
	$O_{def.}$	530.3	17.3	0.34
	$O_{ads.}$	531.5	30.9	
10% Ni-ZnO	$O_{lat.}$	530.1	28.1	
	$O_{def.}$	530.7	27.3	0.97
	$O_{ads.}$	531.5	44.6	
15% Ni-ZnO	$O_{lat.}$	529.7	71.6	
	$O_{def.}$	530.7	22.7	0.32
	$O_{ads.}$	531.6	5.7	
20% Ni-ZnO	$O_{lat.}$	529.9	63.1	
	$O_{def.}$	530.7	29.6	0.47
	$O_{ads.}$	531.6	7.3	
Pure ZnO	$O_{lat.}$	530.9	71.3	
	$O_{def.}$	531.8	22.4	0.31
	$O_{ads.}$	532.7	6.3	

Table S3. Responses of various ZnO-based sensing materials to different concentrations of formaldehyde vapor.

Sensing materials	Concentration (ppm)	Working temperature (°C)	Response	Ref.
3 mol% NiO/ZnO microflowers	100	200	26.2	[45]
CdO-ZnO nanorices	300	350	34.5	[46]
3 wt.% Ag-In$_2$O$_3$/ZnO nanocomposites	100	300	~7.5	[47]
SnO$_2$-ZnO/PdO nanoparticles	10	140	5.3	[48]
ZnO/SnO$_2$ hollow nanospheres	50	225	36.5	[49]
Co$_3$O$_4$/ZnO hollow spheres	10	160	5.8	[50]
1% Er-ZnO nanowires	100	300	~4.7	[51]
10% Ni-ZnO sea urchins	100	200	84.4	This work